Heliyon 10 (2024) e24520

Contents lists available at ScienceDirect

Heliyon

journal homepage: www.cell.com/heliyon

Research article

Mitophagy-related gene signature for predicting the prognosis of multiple myeloma

Tiange Lv [a], Haocong Zhang [b,*]

[a] Cadre's Ward, The General Hospital of Northern Theater Command, Shenyang, Liaoning, 110015, China
[b] Department of Orthopaedics, The General Hospital of Northern Theater Command, Shenyang, Liaoning, 110015, China

ARTICLE INFO

Keywords:
Multiple myeloma
Mitophagy-related genes
Molecular subtypes
Prognostic model
Biomarkers
Survival analysis

ABSTRACT

Aims: The aims of this study were to explore the molecular mechanism of mitophagy in multiple myeloma (MM) and to develop an effective prognostic signature for the disease based on mitophagy-related genes (MRGs).

Methods: Three gene sets from the Reactome database were used to explore MRGs, following which those that were differentially expressed between MM and normal samples were investigated using the data from the Genomic Data Commons–Multiple Myeloma Research Foundation-CoMMpass Study. Mitophagy-related molecular subtypes of MM were identified and their immune infiltration, associated patient survival rates, immune checkpoint genes, and mitophagy scores were compared. Prognostic genes for MM were identified, and a prognostic model was constructed. Additionally, a nomogram was constructed using the prognostic model and prognosis-related clinical features. Finally, the drug sensitivity and correlation analyses of the subtypes were performed between the two risk groups.

Results: We identified two MM molecular subtypes that exhibited significant differences in mitophagy scores, associated patient survival rates, immune infiltration, and immune checkpoint genes. An MRG-based prognostic signature was constructed using six genes (*TRIP13*, *KIF7*, *GPR63*, *CRIP2*, *DNTT*, and *HSPB8*), which had high predictive prognostic value. A nomogram was constructed by screening five indicators (risk score, subtype, age, sex, and stage) that could predict the 1-, 3-, and 5-year survival probabilities of patients with MM. The two risk groups displayed significant differences in their IC_{50} values of 33 drugs, such as bleomycin. Patients in the high-risk group tended to fall within Mitophagy_cluster_A.

Conclusion: Our MRG-based signature is a promising prognostic biomarker for MM.

1. Introduction

Multiple myeloma (MM) is a malignant disease in which plasma cells that synthesize and secrete immunoglobulins become tumorous [1]. Although various therapeutic strategies have been implemented for the clinical treatment of MM, the overall survival (OS) rate of patients remains unsatisfactory [2], with the median survival time after chemotherapy without further intervention being only 7 months [3]. Moreover, the disease has a high recurrence rate [4]. Therefore, exploring the biological mechanisms that affect the

* Corresponding author. Department of Orthopaedics, The General Hospital of Northern Theater Command, No. 83 Wenhua Road, Shenhe District, Shenyang, Liaoning, 110015, China.
E-mail address: Doctorcongcong@163.com (H. Zhang).

https://doi.org/10.1016/j.heliyon.2024.e24520
Received 6 July 2023; Received in revised form 26 November 2023; Accepted 10 January 2024
Available online 13 January 2024
2405-8440/© 2024 The Authors. Published by Elsevier Ltd. This is an open access article under the CC BY-NC-ND license (http://creativecommons.org/licenses/by-nc-nd/4.0/).

pathogenesis of MM is imperative.

Mitophagy (also known as mitochondrial autophagy) is a process in which the number of mitochondria is regulated to correspond to the number of metabolic needs and damaged mitochondria are specifically removed to maintain quality control [5]. In recent years, interest in mitophagy has increased, especially in mitophagy-related genes (MRGs) in human cancers, including MM [6]. A previous study showed that MRGs, including the Unc-51-like kinase 1 (*ULK1*) gene, are critical for the induction of bone metastasis in human cancers via the mitogen-activated protein kinase (MAP2K/MEK) pathway [7]. MRGs are key quality control factors and regulators in human cancer cells [8]. For example, the PTEN-induced kinase 1 (*PINK1*) gene regulates MM cell migration and homing via the Mps one binder kinase activator (MOB1B)-mediated Hippo–Yes-associated protein (YAP)/transcriptional co-activator with PDZ-binding motif (TAZ) pathway [6]. Beider et al. indicated that transient receptor potential vanilloid 1 (TRPV1) contributed to the development of MM by disturbing calcium homeostasis and the bortezomib-induced unfolded protein response [9]. As autophagic markers, genes encoding proteins such as beclin 1 (BECLIN1) and light chain 3 (LC3) have been shown to improve the prognosis and survival of patients with MM [10,11]. A recent study proposed a prognostic model based on 15 autophagy-related genes that could effectively predict the prognosis of patients with MM [12]. Deeper knowledge about the uniquely altered pattern of mitochondrial phagocytosis in MM will enhance our understanding of tumor development and provide innovations for the development of treatment and prognostic strategies for the disease. However, despite advances in the study of mitophagy, an effective and reliable prognostic model for MM based on a comprehensive understanding of mitophagy and MRGs in the tumor tissues is urgently needed.

In this study, we obtained gene expression and clinical data on MM tumor samples from public databases and identified the differentially expressed (DE)-MRGs. After identifying the mitophagy-related molecular subtypes and prognostic genes of MM, a prognostic model for the disease was established. The independent prognostic indicators were analyzed and screened to establish a nomogram. Subsequently, the survival rates of patients in the high- and low-risk groups were identified using the nomogram and its predictive value was evaluated. Finally, drug sensitivity and correlation analyses with the molecular subtypes were performed and compared between the two risk groups. The aims of this study were to elucidate the molecular mechanisms of mitophagy in MM and to develop a promising MRG-based prognostic model for the disease.

2. Materials and methods

The workflow of this study is depicted in Supplementary Fig. S1.

2.1. Microarray data

Clinical information (patient age, patient sex, tumor stage, family history, disease type, OS, and OS time) and RNA-Seq data (log2 (count+1) and fragments per kilobase of transcript per million mapped reads (FPKM)) from the Genomic Data Commons–Multiple Myeloma Research Foundation-CoMMpass (GDC MMRF-CoMMpass) Study were downloaded from the University of California Santa Cruz Xena database [13]. After filtering the cases with an OS of less than 30 days, a total of 774 MM samples (MM group) were retained for the analysis. For external validation, the microarray dataset GSE2658 in the Gene Expression Omnibus (GEO) database [14] was used. This dataset comprises 599 tumor samples, each of which has accompanying survival information (Platform: GPL570 Affymetrix Human Genome U133 Plus 2.0 Array). Probes lacking gene symbol matches were eliminated on the basis of their annotation file. For genes with multiple corresponding probes, the average value was used. Additionally, 755 normal blood samples (N group) were downloaded from the GTEx database (https://www. gtexportal. org/) for subsequent analysis.

2.2. Differentially expressed mitophagy-related gene investigation and correlation analysis

Three MRG sets (R-HSA-5205685.3, R-HSA-5205647.4, and R-HSA-8934903.3) were screened from the Reactome database (https://reactome.org/), and the MRGs in common among them were revealed through intersection analysis. Then, the differential expression of those MRGs between the MM and N groups was analyzed, and the DE-MRGs were investigated using the *t*-test and DESeq2 tool. Finally, correlation analysis between the DE-MRGs in the GDC MMRF-CoMMpass samples was performed using the ggcor package (version 0.9.8.1) in R [15].

2.3. Prediction and rationality validation of mitophagy-related subtypes of multiple myeloma and analysis of their correlation with clinical characteristics

Unsupervised clustering of the patients with MM on the basis of MRGs was performed using the ConsensusClusterPlus package (version 1.60.0) in R [16]. The enrichment score of the REACTOME_MITOPHAGY (C2 CP) mitochondrial autophagy pathway in all samples was calculated using gene set variation analysis (GSVA, version 1.44.2) [17]. The enrichment scores of mitophagy pathways were compared between the subtypes using Student's t-test. Moreover, to reveal the difference in prognosis between the molecular subtypes, Kaplan–Meier (K–M) survival analysis was performed using the survival package (version 3.4) in R [18]. Finally, the relationships between the 28 MRGs and clinical characteristics (including age, sex, stage, molecular subtype, mitophagy-related pathway enrichment score, and OS time) were investigated.

2.4. Analysis of immune cell infiltration in the molecular subtypes of multiple myeloma

To reveal the relationship between mitochondrial autophagy molecular subtypes and the tumor microenvironment, the algorithms ESTIMATE [19], CIBERSORT [20], and ssGSEA [17] were used to evaluate the immune microenvironment state of the GDC MMRF-CoMMpass samples. The immune cell infiltration levels among the molecular subtypes were compared using Wilcoxon's signed-rank test.

2.5. Analysis of immune checkpoint and human leukocyte antigen genes among the subtypes

The expression levels of 48 immune checkpoint and 18 human leukocyte antigen (*HLA*) genes in the GDC MMRF-CoMMpass dataset were determined. The difference in expression between the mitophagy-related subtypes was revealed using Wilcoxon's signed rank test.

2.6. Revealing differentially expressed genes among the subtypes

The DEGs between the molecular subtypes identified from the GDC MMRF-CoMMpass dataset were explored using the DESeq2 package (version 1.36.0) in R [21]. The DEG selection thresholds were a false discovery rate (calculated using the Benjamini–Hochberg method [22]) of less than 0.05 and a $|\log_2$ fold change$|$ of greater than 1.

2.7. Definitions of the training, testing, and external verification datasets

The data (FPKM) of the tumor samples in the GDC MMRF-CoMMpass Study were randomly partitioned into training and testing datasets at a ratio of 6:4. GEO data (log2(exp+1)) were used as an external verification set. The training dataset was used to establish the prognostic model, and the testing and external verification sets were used to confirm the model effectiveness.

2.8. Prognostic gene investigation

Prognostic genes related to OS were identified by investigating the relationships between the expression levels of DEGs and prognostic information of the samples, using univariate Cox regression analysis. The survival package (version 2.41-1) in R [23] was used to conduct this analysis.

2.9. Prognostic model establishment

From the prognostic DEGs, the optimal gene set for model establishment was selected through LASSO Cox regression analysis using the glmnet package (version 2.0-18) in R (version 3.6.1) [24]. A 10-fold cross-validation analysis was performed. Finally, the model was constructed using Equation (1):

$$\text{Risk score} = \sum \beta_{\text{gene}} \times \text{Exp}_{\text{gene}} \tag{1}$$

where β_{gene} represents the Cox regression-derived prognostic coefficient pertaining to each MRG, and Exp_{gene} represents the MRG expression in the GDC MMRF-CoMMpass training dataset.

2.10. Prognostic model validation

To validate the prognostic model, the median risk score of samples in the GDC MMRF-CoMMpass testing dataset and external verification dataset (GSE2658) was calculated. All samples were then separated into high- and low-risk groups. K–M curves were plotted using the survival package in R [18][18] to analyze survival differences between the two risk groups. Additionally, the area under the receiver operating characteristic (ROC) curve (AUC) was used to evaluate the performance of the prognostic model in predicting patient survival.

2.11. Independent analysis of the prognostic model

Univariate and multivariate Cox regression analyses were used to assess the independence of the prognostic model from clinical factors, such as subtype, age, sex, and stage. The cutoff value was a log-rank *P* value of less than 0.05. Factors with independent prognoses were used to establish the nomogram, using the rms package in R [25]. On the basis of the independent prognostic factors, a clinical risk model was constructed, and the clinical risk value nomoScore of all GDC MMRF-CoMMpass samples was calculated. All GDC MMRF-CoMMpass samples were divided into high-nomoRisk and low-nomoRisk groups. The prognosis of these two groups was compared using K–M curve analysis, and the prognostic value of the clinical risk model was evaluated using the ROC curve. To assess the performance of the nomogram, calibration curve analysis and decision curve analysis (DCA) were conducted using the rms and dcurves packages [25] in R, respectively.

2.12. Drug sensitivity analysis

The Cancer Drug Sensitivity Genomics database was used to estimate the sensitivity of each patient to various chemotherapy drugs. The difference in sensitivity (i.e., inhibitory concentration 50 (IC_{50}) value) of the chemotherapy drugs was quantified using the pRRophic algorithm [26]. Then, Wilcoxon's signed rank test was used to compare the IC_{50} value of each drug between the two risk groups.

2.13. Analysis of the correlation between the multiple myeloma subtypes and different risk groups

The correlations between the different risk groups and MM subtypes were analyzed using the chi-squared test. The subtype distribution in the risk groups was visualized as a bar chart.

2.14. Statistical analysis

R software (version 4.2.1) was used for all statistical analyses. Differences with a *P* value of less than 0.05 were considered statistically significant.

3. Results

3.1. Differentially expressed mitophagy-related genes in multiple myeloma

In total, 29 MRGs in common were obtained through intersection analysis of three sets of MRGs. Differential expression analysis

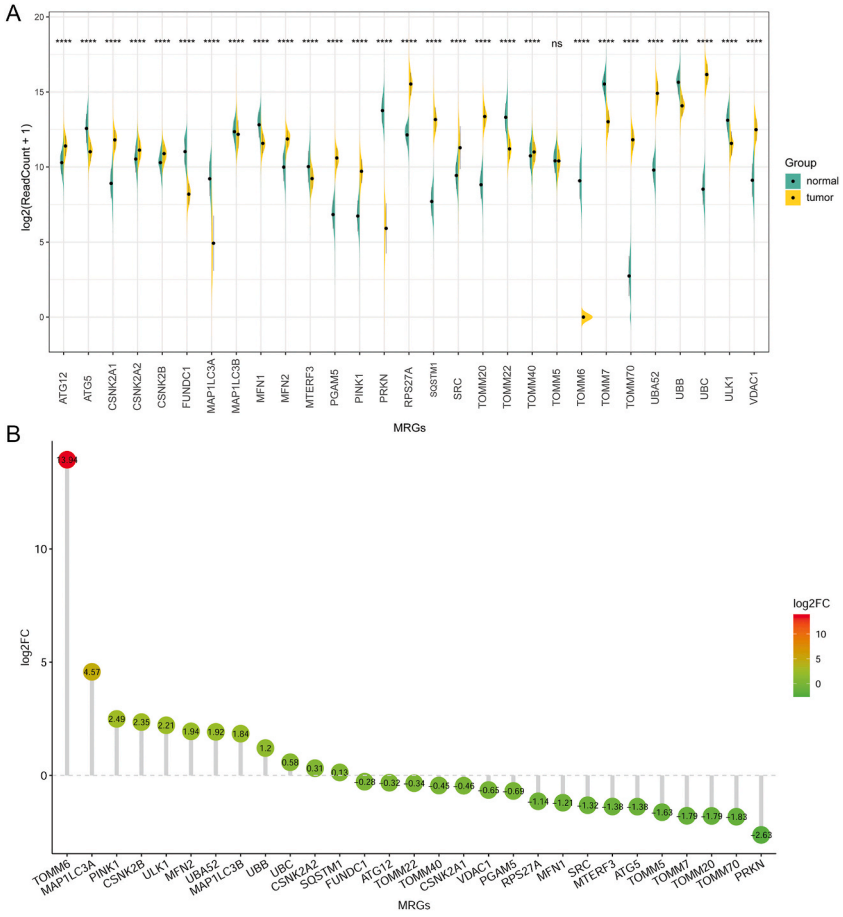

Fig. 1. Analysis of mitophagy-related genes (MRGs) that are differentially expressed between multiple myeloma (MM) and normal samples. A, The *t*-test reveals the difference in expression of 29 MRGs between the MM and normal samples: green represents normal samples, and yellow represents MM samples. B, DESeq2 reveals 9 upregulated and 10 downregulated MRGs: the height of the column represents the fold change. (For interpretation of the references to colour in this figure legend, the reader is referred to the Web version of this article.)

showed that, except for *TOMM5*, 28 MRGs were differentially expressed between the MM and N groups (Fig. 1A). DESeq2 analysis revealed 9 upregulated (*MFN2*, *MAP1LC3A*, *MAP1LC3B*, *TOMM6*, *PINK1*, *UBB*, *UBA52*, *ULK1*, and *CSNK2B*) and 10 downregulated MRGs (*ATG5*, *MFN1*, *MTERF3*, *TOMM70*, *TOMM20*, *TOMM7*, *TOMM5*, *PRKN*, *RPS27A*, and *SRC*) (Fig. 1B). Additionally, correlation analysis of the genes in the GDC MMRF-CoMMpass dataset showed co-expression between MRGs (Supplementary Fig. S2).

3.2. Mitophagy-related subtypes of multiple myeloma and their correlation with clinical characteristics

Unsupervised clustering based on the DE-MRGs revealed two molecular subtypes; namely, Mitophagy_cluster_A (473 patients) and Mitophagy_cluster_B (301 patients) (Fig. 2A–C). The *t*-test indicated a significantly higher mitophagy enrichment score in Mitophagy_cluster_B than in Mitophagy_cluster_A ($P < 0.01$) (Fig. 2D). Moreover, K–M analysis showed that patients in Mitophagy_cluster_B had a higher survival probability than those in Mitophagy_cluster_A ($P < 0.01$) (Fig. 2E). The correlation between the DE-MRGs and clinical characteristics is shown in Supplementary Fig. S3.

3.3. Differences in immune cell infiltration between the two mitophagy-related subtypes

The difference in immune cell infiltration between the two mitophagy-related subtypes was investigated. The ssGSEA results revealed that 16 types of immune cells, including regulatory T cells, were significantly different between the two subtypes (all $P < 0.01$) (Fig. 3A). Moreover, the CIBERSORT analysis results revealed that the percentage of neutrophils and activated natural killer cells was significantly higher in Mitophagy_cluster_B than in Mitophagy_cluster_A (all $P < 0.01$) (Fig. 3B). Furthermore, according to the ESTIMATE analysis results, Mitophagy_cluster_A had significantly higher ESTIMATE scores, ImmuneScores, and StromalScores than Mitophagy_cluster_B (all $P < 0.01$) (Fig. 3C).

3.4. Differences in immune checkpoint and HLA gene expression between the two mitophagy-related subtypes

Except for *TNFRSF4*, *TNFPSF18*, *NRP1*, *LAIR1*, *LAG3*, *KIR3DL1*, *CD276*, *CD27*, and *CD200R1*, 29 other immune checkpoint genes showed differential expression when comparing the two subtypes (Fig. 4A). For example, the patients in Mitophagy_cluster_B

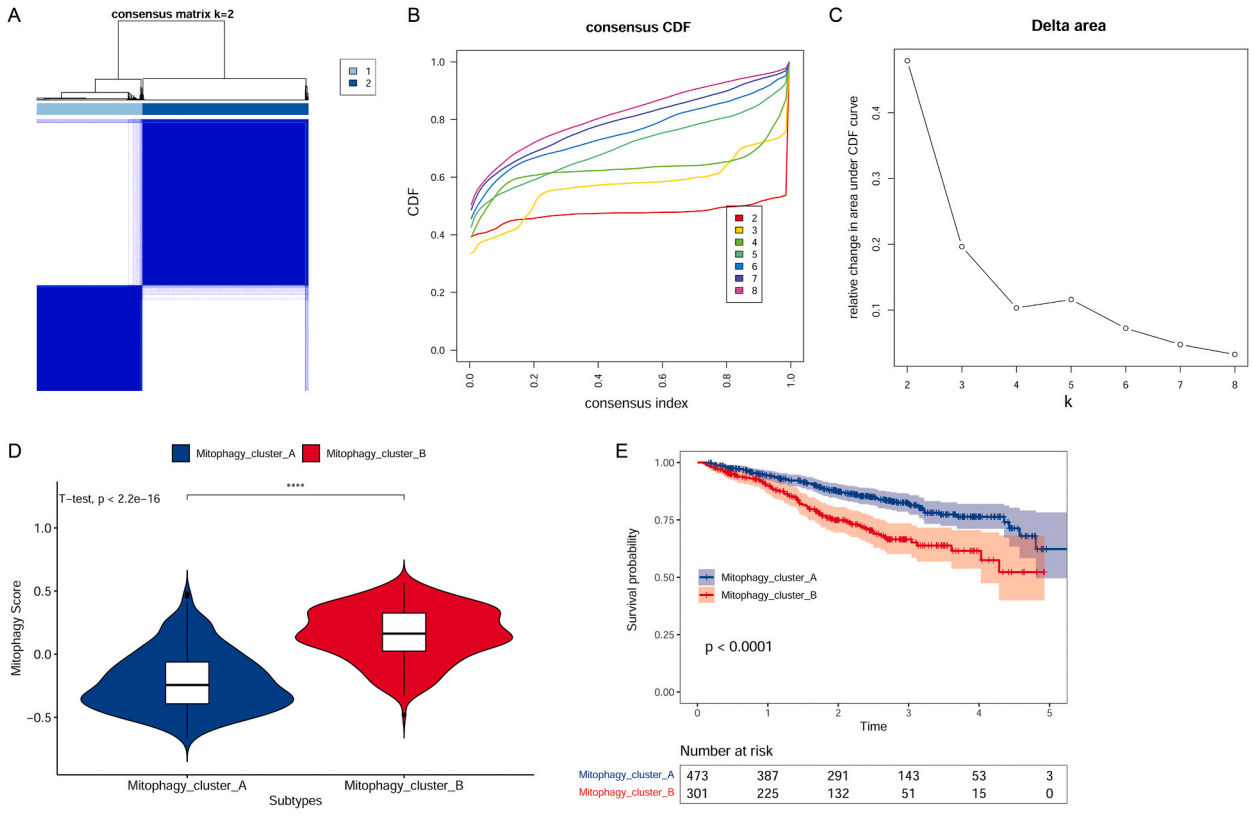

Fig. 2. Mitophagy-related molecular subtypes of multiple myeloma (MM), rationality verification, and correlation with clinical characteristics. A, Consensus matrix showing K = 2. B, Consensus cumulative density function (CDF) under different K values. C, Delta area of each K value. D, Violin chart showing the mitophagy score of the two MM subtypes: the X-axis represents the MM clusters, and the Y-axis represents the mitophagy score. E, Kaplan–Meier (K–M) survival curve showing the survival probability of the two MM subtypes.

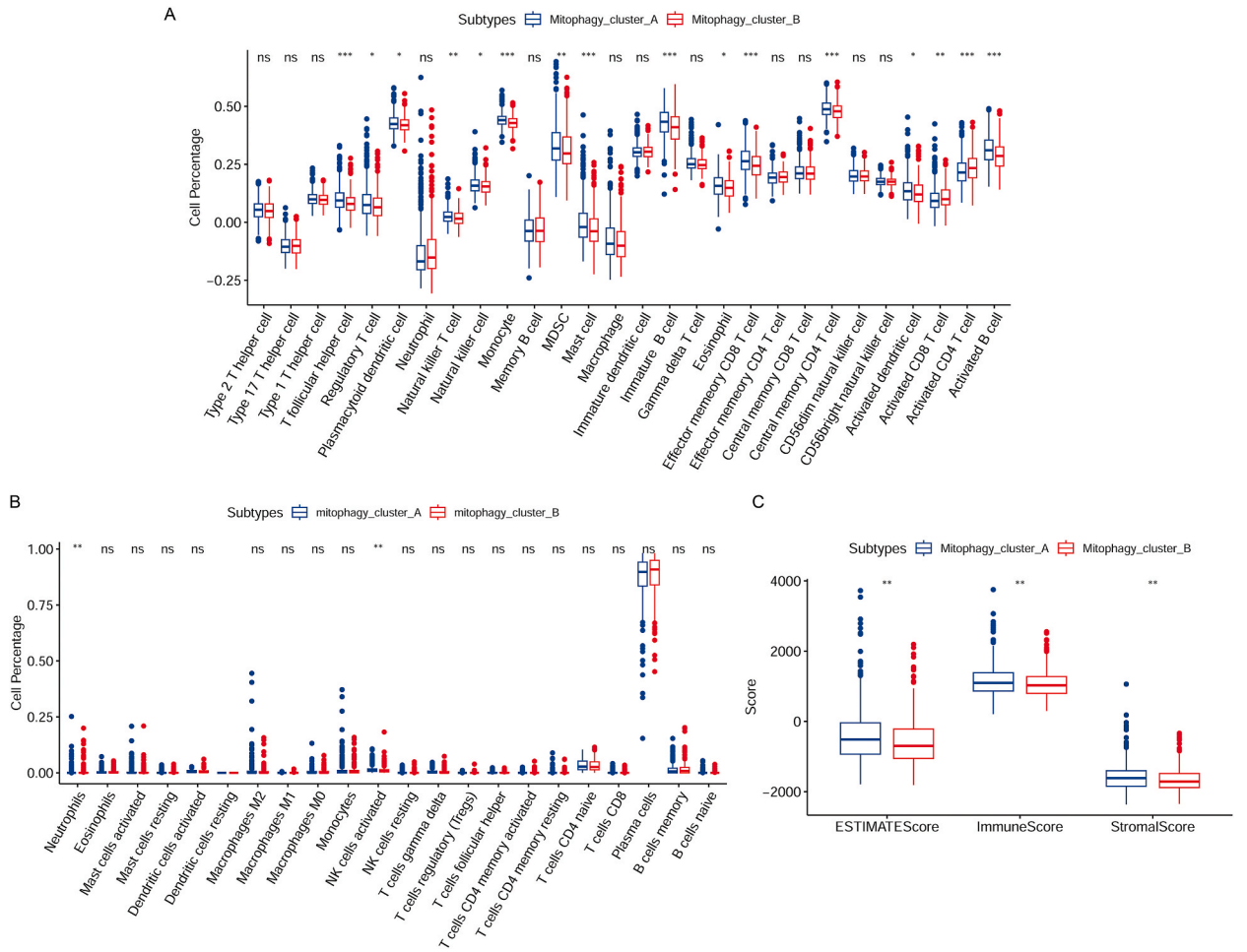

Fig. 3. Immune cell infiltration in the two mitophagy-related molecular subtypes of multiple myeloma (MM). A, ssGSEA analysis showing immune cell infiltration differences between the two subtypes. B, CIBERSORT results revealing the difference in immune cell infiltration between the two subtypes. C, ESTIMATE results revealing the difference in immune cell infiltration between the two subtypes. **, $P < 0.05$; ***, $P < 0.01$; ns, not significant.

expressed significantly higher levels of *TIGIT* and *CD40* than those in Mitophagy_cluster_A ($P < 0.01$). Furthermore, the expression levels of HLA genes (including *HLA-E*, *HLA-F*, *HLA-DOB*, *HLA-DMA*, *HLA-C*, *HLA-B*, and *HLA-A*) in Mitophagy_cluster_A were significantly higher than those in Mitophagy_cluster_B (all $P < 0.05$) (Fig. 4B).

3.5. Prognostic model construction and validation

The DEGs of the GDC MMRF-CoMMpass dataset were further investigated using DESeq2, revealing 364 DEGs between the two molecular subtypes (Supplementary Fig. S4). Univariate Cox regression analysis based on the training dataset revealed 46 DEGs related to OS in MM ($P < 0.05$). Of these, 16 genes were identified to have prognostic value according to LASSO Cox regression analysis (Supplementary Fig. S5A). Multivariate regression analysis identified six optimal prognostic signatures; that is, four upregulated (*TRIP13*, *KIF7*, *GPR63*, and *CRIP2*) and two downregulated genes (*DNTT* and *HSPB8*). A prognostic model was then constructed on the basis of these genes (Supplementary Fig. S5B). Additionally, the samples were stratified by two risk groups (Fig. 5A), whereupon the high-risk group was found to have worse survival than the low-risk group ($P > 0.01$). The results of the ROC curve analysis for 1-year (AUC = 0.737), 3-year (AUC = 0.684), and 5-year survival (AUC = 0.643) are shown in Fig. 5B. Furthermore, the prognosis difference was significant between the two risk groups in both the GDC MMRF-CoMMpass testing dataset (Fig. 5C) and GEO external verification dataset (all $P < 0.05$) (Fig. 5D). The ROC survival curves for the two datasets demonstrated the high predictive value of the constructed prognostic model (Fig. 5E and F).

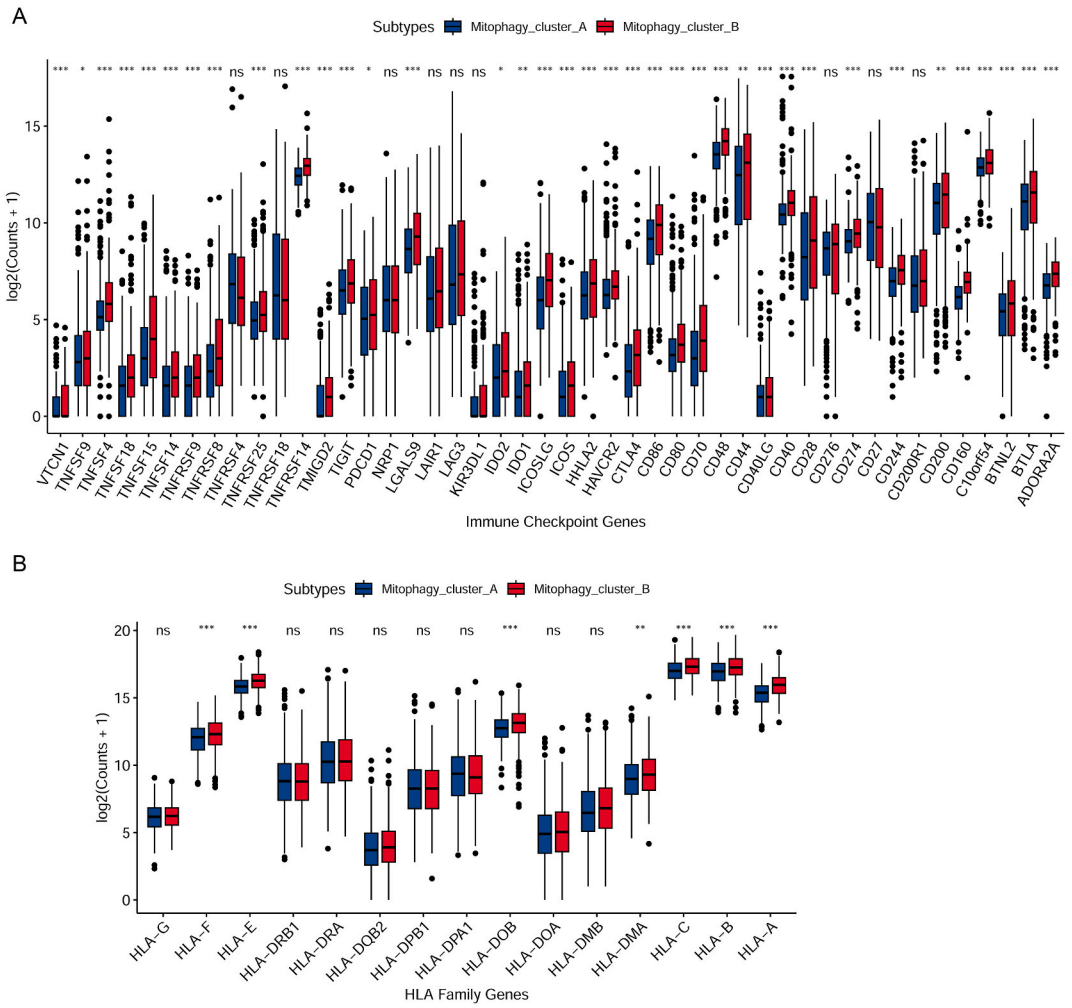

Fig. 4. Differences in immune checkpoint and *HLA* gene expression between the two mitophagy-related molecular subtypes of multiple myeloma (MM). A, Difference in immune checkpoint gene expression between the two subtypes. B, Difference in *HLA* family gene expression between the two subtypes. **, $P < 0.05$; ***, $P < 0.01$; ns, not significant.

3.6. Independent analysis of the prognostic model

Univariate and multivariate Cox regression analyses revealed five independent prognostic factors: risk score, subtype, age, sex, and stage (Fig. 6A–B). Subsequently, a nomogram was constructed to predict the 1-, 3-, and 5-year survival probabilities of patients with MM (Fig. 6C).

Based on the different risk groups determined from the median of the nomoscore, K–M survival analysis of the GDC MMRF-CoMMpass dataset showed that patients with a high nomoscore had a worse prognosis than those with a low nomoscore (Fig. 6D). The AUC at 1-, 3-, and 5-years were 0.751, 0.762, and 0.726, respectively (Fig. 6E). The DCA and calibration curve analysis of the nomogram indicated that the predicted survival rates at 1, 3, and 5 years were highly accurate (Fig. 6F–H).

3.7. Drug sensitivity and subtype distribution in the two risk groups

The sensitivity (IC_{50} values) of the two risk groups to 129 drugs was compared, revealing significant differences in the IC_{50} values of 33 drugs (all $P < 0.01$). For example, the IC_{50} value of bleomycin was higher in the high-risk group (Fig. 7A), whereas that of bicalutamide was higher in the low-risk group (Fig. 7B). Moreover, the correlation analysis revealed that patients in the high-risk group tended to fall within Mitophagy_cluster_A, whereas those in the low-risk group mostly belonged to Mitophagy_cluster_B (Fig. 7C).

4. Discussion

MM is the second most common hematologic malignancy worldwide and generally has a poor prognosis [27]. Although autophagy

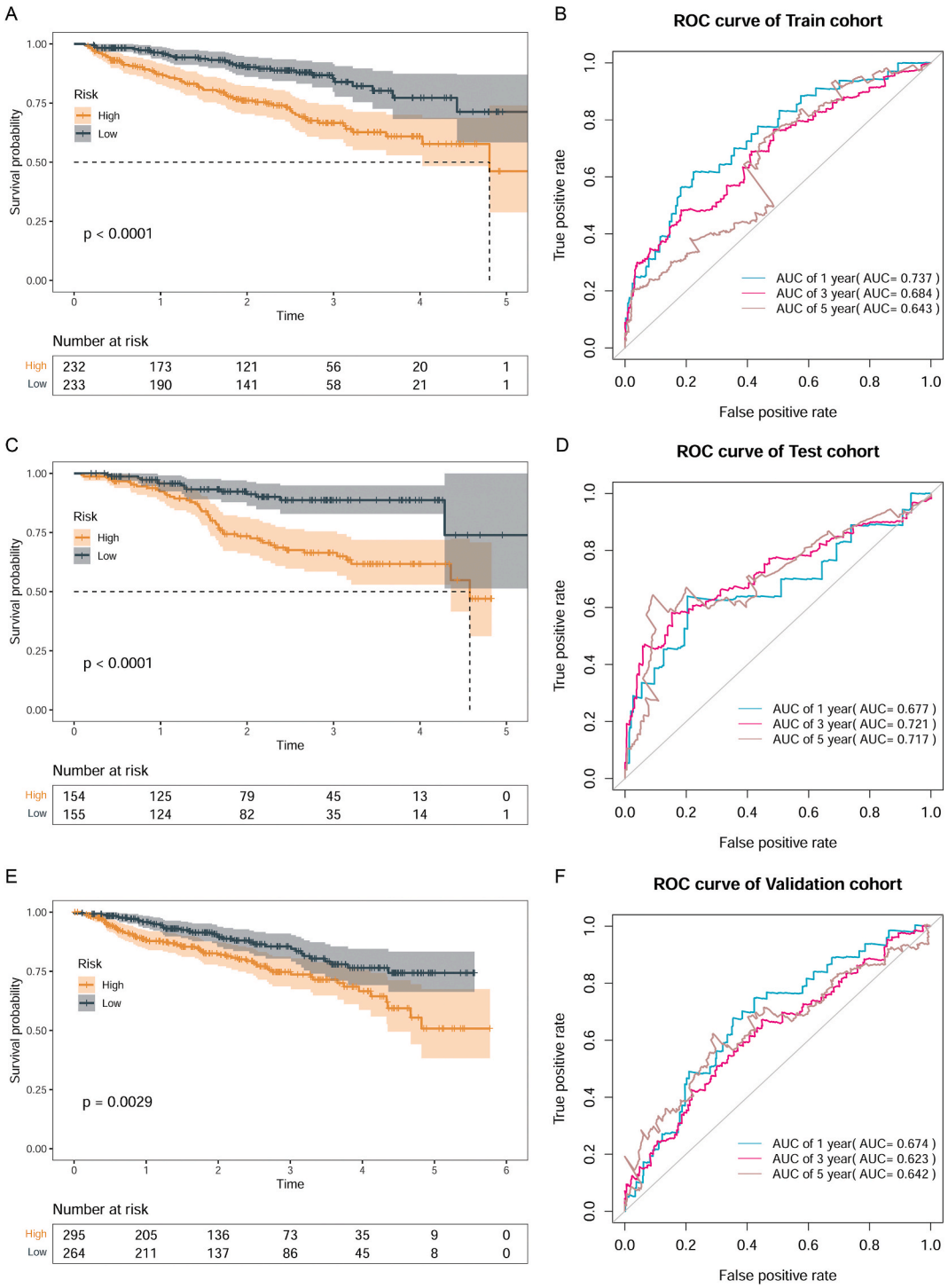

Fig. 5. Predictive value of the prognostic model. A, Kaplan–Meier (K–M) survival curves of samples stratified by the risk score model in the training dataset. B, Receiver operating characteristic (ROC) curves showing the value of the model in predicting 1-, 3-, and 5-year survival based on samples in the training dataset. C, K–M survival curves of samples stratified by the model in the testing dataset. D, ROC curves based on samples in the test dataset. E, K–M survival curves of samples stratified by the model in the external verification dataset. F, ROC curves based on the external verification dataset.

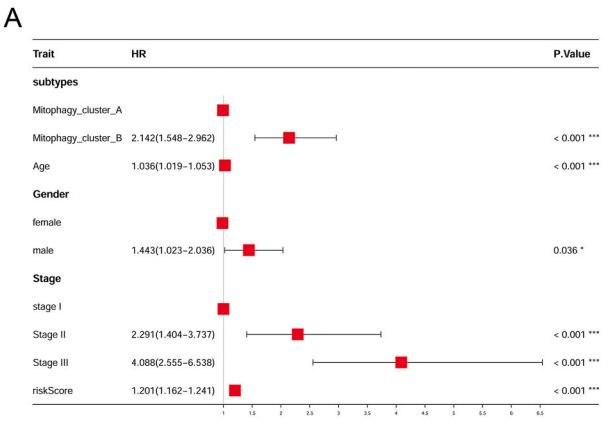

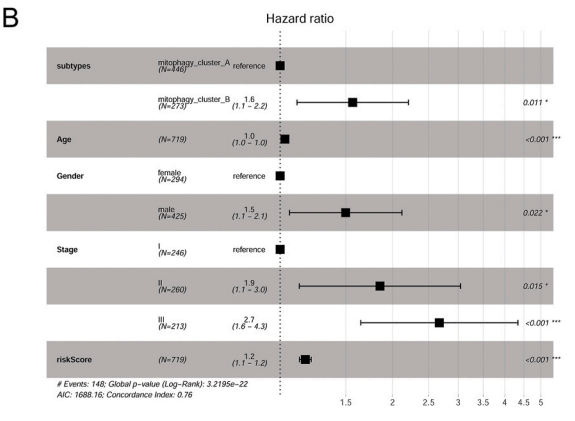

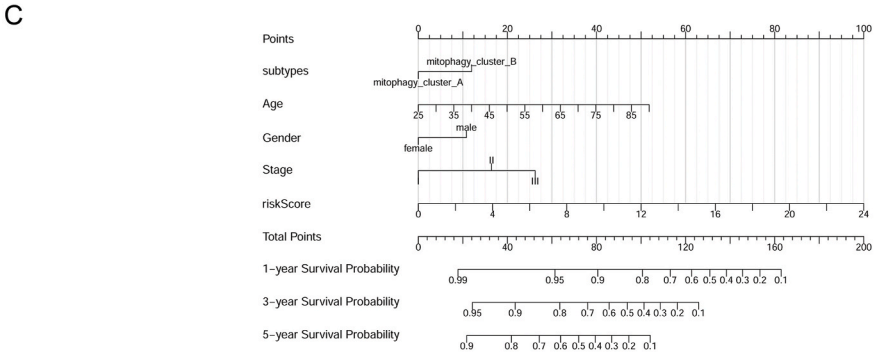

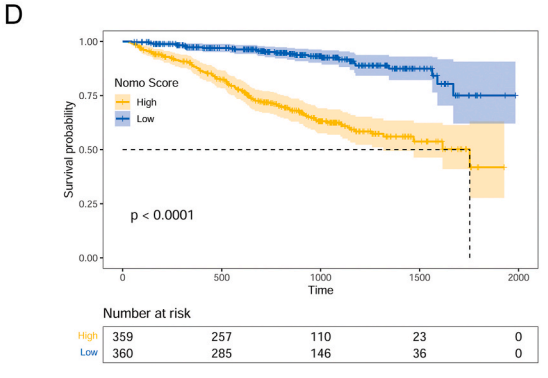

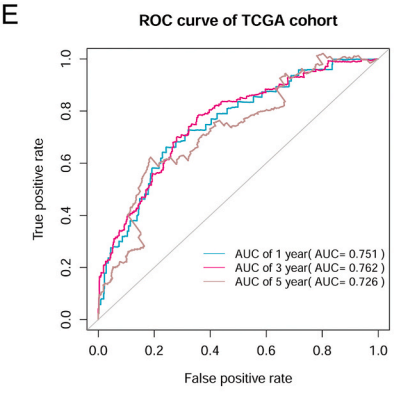

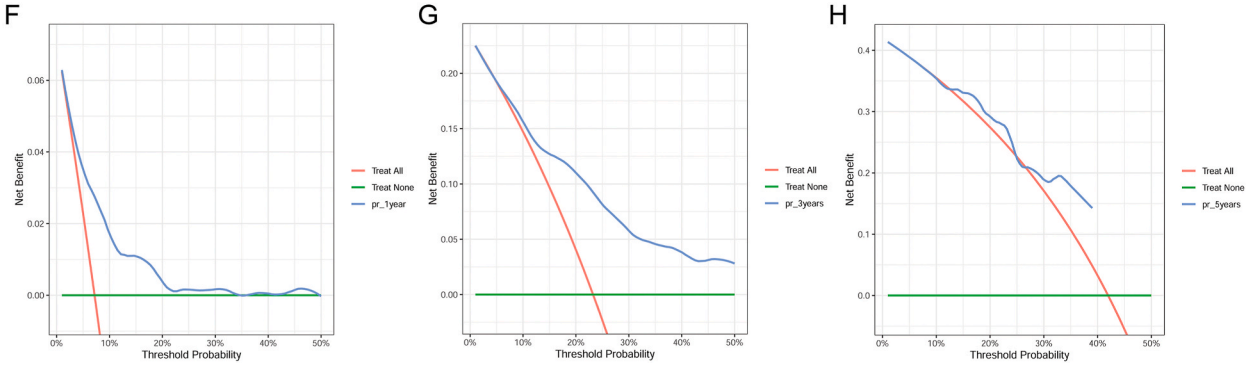

(caption on next page)

Fig. 6. Investigation of prognostic factors for multiple myeloma (MM). A, Univariate regression for clinical factors (risk score, subtype, age, sex, stage) and prognosis. B, Multivariate regression revealing the independent factors for MM. C, Constructed nomogram for predicting the overall survival (OS) of patients with MM. D, Kaplan–Meier survival analysis of samples stratified by the nomogram based on the whole GDC MMRF-CoMMpass dataset. E, Receiver operating characteristic curves based on samples in the whole GDC MMRF-CoMMpass dataset. F–H, Results of 1-, 3-, and 5-year decision curve analysis (DCA).

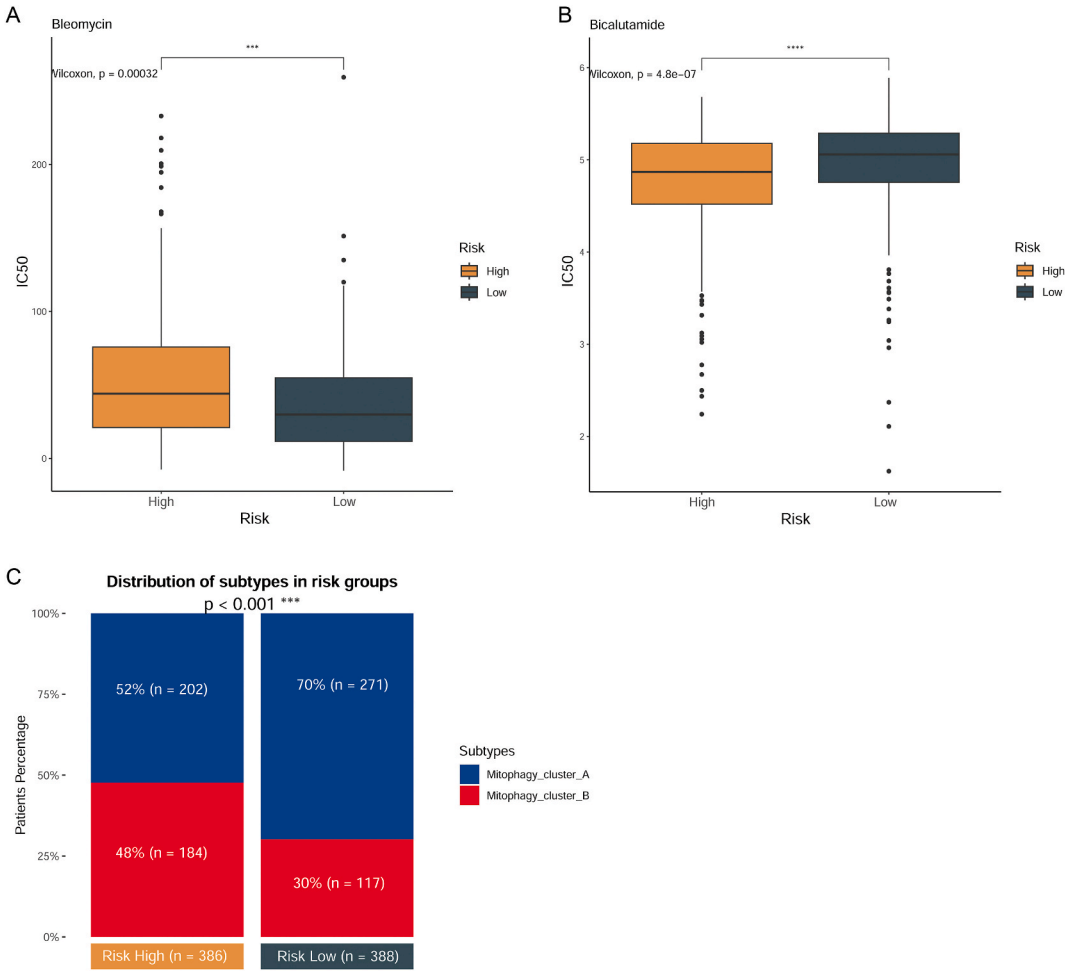

Fig. 7. Drug sensitivity and mitophagy-related molecular subtype distribution of the two risk groups. A, Difference in the inhibitory concentration 50 (IC_{50}) of bleomycin between the two risk groups. B, Difference in the IC_{50} of bicalutamide between the two risk groups. C, Distribution of the subtypes in the two risk groups.

is essential in the development and prognosis of various cancers, including MM [28], the detailed molecular mechanisms of mitophagy in MM remain unclear. In this study, we investigated the mitophagy-related molecular subtypes of MM and constructed an MRG-based prognostic signature, providing a reference basis for future studies on the early diagnosis and treatment of the disease.

Autophagy plays a vital role in inflammation, the immune response, and drug resistance in MM [29]. As an immune checkpoint gene, *CD28* mediates pro-survival autophagy signaling, which induces chemotherapy resistance in patients with MM [30]. CD80, a ligand of CD28, is vital for immunotherapy of human cancers, including MM [31]. High levels of neutrophils in the bone marrow promote chemoresistance in patients with MM [32]. The antineoplastic drug bleomycin can induce lung injury, leading to the production of a high number of neutrophils [33]. A study examining the neutrophil/lymphocyte ratio in patients with MM demonstrated a significant elevation in neutrophil count, indicating a correlation between high numbers of neutrophils and MM development [34]. These differences in immune response and inflammation are important indicators of different human cancer subtypes. It has been shown that the definition of autophagy-related gene expression can be used to define subtypes with different clinical and microenvironmental cell infiltration characteristics [35]. Zhang et al. indicated that molecular subtypes of MM are associated with prognostic significance, laying an important foundation for subsequent treatment [36]. In this study, two mitophagy-related subtypes of MM were identified on the basis of DE-MRGs between disease and control samples. Immune cells, including neutrophils, and immune checkpoint

genes, such as *CD28* and *CD80*, were significantly differentially expressed between the two subtypes. Correlation analysis of survival and clinical characteristics revealed a clear distinction between patients with different subtypes. Thus, we speculated that the MRG classification could be used to define MM subtypes.

Owing to the interactions between regulators of mitochondrial phagocytosis, mitophagy has been implicated in innate immunity, inflammation, and tumor progression [37]. In this study, the prognostic model constructed using six DEGs (viz., *TRIP13*, *KIF7*, *GPR63*, *CRIP2*, *DNTT*, and *HSPB8*) demonstrated good predictive ability in MM. Thyroid hormone receptor interactor 13 (TRIP13), which is a critical regulator of mitosis, is commonly upregulated in human tumor cell lines and tissues and is closely linked to tumor progression and poor prognosis [38]. Kinesin family member 7 (KIF7) is a crucial molecular motor protein that participates in mitosis and cell cycle progression [39]. Differential expression of KIF7 contributes to prostate cancer development [40]. G-protein-coupled receptor 63 (GPR63), a member of the transmembrane signaling molecule superfamily, is commonly upregulated in tumor cells [41]. A previous study showed that GPR63 is a promising biomarker overexpressed in proliferating cells [42]. DNA nucleotidylexotransferase (DNTT) is involved in DNA repair [43]. Heat shock protein family B [small] member 8 (HSPB8), a small chaperone that promotes the selective degradation of proteins [44], has been shown to participate in the development of drug resistance [45]. Hamouda et al. indicated that resistance to bortezomib in MM is mediated by the autophagic clearance of misfolded proteins induced by HSPB8 overexpression [46].

With regard to drug sensitivity, the high-risk patients in this study were associated with poor survival and high IC_{50} values for drugs such as bleomycin. It has been reported that the sensitivity to chemotherapy drugs can be used to determine the clinical outcomes of patients [47]. Bleomycin is a glycopeptide antibiotic that is used in combination with chemotherapy [48]. A previous study on colon cancer showed that the high-risk group identified by a ferroptosis-related long noncoding RNA signature exhibited lower IC_{50} values for certain chemotherapeutic drugs, such as bleomycin [49], suggesting that analyzing the drug sensitivity of different risk groups can guide the design of personalized treatment. The results of our study indicated that a mitophagy-related prognostic signature can predict the survival of patients with MM. Genes such as *TRIP13*, *KIF7*, *GPR63*, *CRIP2*, *DNTT*, and *HSPB8* may be novel prognostic markers for this disease.

Nomograms are widely used as predictive tools in oncology and medicine [50] and are also being commonly applied to explore the risk of human cancers [51]. A pleural effusion-based nomogram constructed by Hou et al. outperformed the Durie–Salmon and international staging systems in accurately stratifying patients with MM into different risk groups [52]. In another study, a nomogram was successfully established to predict the OS of patients with newly diagnosed MM [53]. It has been proved that age, sex, and stage are independent predictors of survival for patients with MM [54]. Wang et al. indicated that age and risk score were independent prognostic predictors of MM in their constructed nomogram [55]. Our nomogram based on risk score, subtype, age, sex, and stage could accurately predict the 1-, 3-, and 5-year survival probabilities of patients with MM, as verified by the DCA and calibration curve. Thus, we conclude that this novel nomogram is valuable in predicting the survival of patients with this disease.

This study has several limitations. First, the expression and regulatory mechanisms of key MRGs have not yet been experimentally validated. Second, the mitophagy-related prognostic signature was constructed and validated using publicly available data. Its prognostic value should be validated in a clinical setting.

5. Conclusion

In summary, we have developed a mitophagy-related prognostic signature that can independently predict the survival of patients with MM. The MRG classification may be used to define subtypes of MM with distinct clinical and microenvironmental cell infiltration characteristics. *TRIP13*, *KIF7*, *GPR63*, *CRIP2*, *DNTT*, and *HSPB8* may serve as novel biomarkers of MM prognosis.

Data availability

The data supporting the findings of this study are available from the corresponding author upon reasonable request.

Funding

This work was supported by “Clinical study of shear-wave elastography accurately determining degenerative scoliosis-fixed segments” (Program No. 2022020785-JH2/1015).

CRediT authorship contribution statement

Tiange Lv: Writing – original draft, Conceptualization. **Haocong Zhang:** Writing – review & editing, Conceptualization.

Declaration of competing interest

The authors declare that they have no known competing financial interests or personal relationships that could have appeared to influence the work reported in this paper.

Acknowledgements

None.

Appendix A. Supplementary data

Supplementary data to this article can be found online at https://doi.org/10.1016/j.heliyon.2024.e24520.

References

[1] A. Mahindra, T. Hideshima, K.C. Anderson, Multiple myeloma: biology of the disease, Blood Rev. 24 (2010) S5–S11.
[2] J. Mikhael, Treatment Options for Triple-class Refractory multiple myeloma, Clin Lymphoma Myeloma Leuk 20 (2020) 1–7.
[3] A.J. Cowan, D.J. Green, M. Kwok, S. Lee, D.G. Coffey, L.A. Holmberg, S. Tuazon, A.K. Gopal, E.N. Libby, Diagnosis and management of multiple myeloma: a review, JAMA 327 (2022) 464–477.
[4] N. van de Donk, C. Pawlyn, K.L. Yong, Multiple myeloma, Lancet 397 (2021) 410–427.
[5] M. Onishi, K. Yamano, M. Sato, N. Matsuda, K. Okamoto, Molecular mechanisms and physiological functions of mitophagy, Embo j 40 (2021) e104705.
[6] S. Fan, T. Price, W. Huang, M. Plue, J. Warren, P. Sundaramoorthy, B. Paul, D. Feinberg, N. MacIver, N. Chao, D. Sipkins, Y. Kang, PINK1-Dependent mitophagy regulates the migration and homing of multiple myeloma cells via the MOB1B-mediated hippo-YAP/TAZ pathway, Adv. Sci. 7 (2020) 1900860.
[7] R. Deng, H.L. Zhang, J.H. Huang, R.Z. Cai, Y. Wang, Y.H. Chen, B.X. Hu, Z.P. Ye, Z.L. Li, J. Mai, Y. Huang, X. Li, X.D. Peng, G.K. Feng, J.D. Li, J. Tang, X.F. Zhu, MAPK1/3 kinase-dependent ULK1 degradation attenuates mitophagy and promotes breast cancer bone metastasis, Autophagy 17 (2021) 3011–3029.
[8] C.W. Yun, J. Jeon, G. Go, J.H. Lee, S.H. Lee, The dual role of autophagy in cancer development and a therapeutic strategy for cancer by targeting autophagy, Int. J. Mol. Sci. 22 (2020) 179.
[9] K. Beider, E. Rosenberg, V. Dimenshtein-Voevoda, Y. Sirovsky, J. Vladimirsky, H. Magen, O. Ostrovsky, A. Shimoni, Z. Bromberg, L. Weiss, A. Peled, A. Nagler, Blocking of Transient Receptor Potential Vanilloid 1 (TRPV1) promotes terminal mitophagy in multiple myeloma, disturbing calcium homeostasis and targeting ubiquitin pathway and bortezomib-induced unfolded protein response, J. Hematol. Oncol. 13 (2020) 158.
[10] R. Bútová, P. Vychytilová-Faltejsková, J. Gregorová, L. Radová, M. Almáši, R. Bezděková, L. Brožová, J. Jarkovský, Z. Knechtová, M. Štork, LncRNAs LY86-AS1 and VIM-AS1 distinguish plasma cell leukemia patients from multiple myeloma patients, Biomedicines 9 (2021) 1637.
[11] T. Chen, T. Berno, M. Zangari, Low-risk identification in multiple myeloma using a new 14-gene model, Eur. J. Haematol. 89 (2012) 28–36.
[12] Y. Qiu, H.T. Wang, X.F. Zheng, X. Huang, J.Z. Meng, J.P. Huang, Z.P. Wen, J. Yao, Autophagy-related long non-coding RNA prognostic model predicts prognosis and survival of melanoma patients, World J Clin Cases 10 (2022) 3334–3351.
[13] M.J. Goldman, B. Craft, M. Hastie, K. Repečka, F. McDade, A. Kamath, A. Banerjee, Y. Luo, D. Rogers, A.N. Brooks, J. Zhu, D. Haussler, Visualizing and interpreting cancer genomics data via the Xena platform, Nat. Biotechnol. 38 (2020) 675–678.
[14] R. Edgar, M. Domrachev, A.E. Lash, Gene Expression Omnibus: NCBI gene expression and hybridization array data repository, Nucleic Acids Res. 30 (2002) 207–210.
[15] H. Huang, L. Zhou, J. Chen, T. Wei, ggcor: extended tools for correlation analysis and visualization, R package (2020). https://gitee.com/dr_yingli/ggcor#citation. version 0.9.7.
[16] M.D. Wilkerson, D.N. Hayes, ConsensusClusterPlus: a class discovery tool with confidence assessments and item tracking, Bioinformatics 26 (2010) 1572–1573.
[17] S. Hänzelmann, R. Castelo, J. Guinney, GSVA: gene set variation analysis for microarray and RNA-seq data, BMC Bioinf. 14 (2013) 7.
[18] T.M. Therneau, T. Lumley, Package 'survival', R Top Doc 128 (10) (2015) 28–33, 6.
[19] K. Yoshihara, M. Shahmoradgoli, E. Martínez, R. Vegesna, H. Kim, W. Torres-Garcia, V. Treviño, H. Shen, P.W. Laird, D.A. Levine, S.L. Carter, G. Getz, K. Stemke-Hale, G.B. Mills, R.G. Verhaak, Inferring tumour purity and stromal and immune cell admixture from expression data, Nat. Commun. 4 (2013) 2612.
[20] B. Chen, M.S. Khodadoust, C.L. Liu, A.M. Newman, A.A. Alizadeh, Profiling tumor infiltrating immune cells with CIBERSORT, Methods Mol. Biol. 1711 (2018) 243–259.
[21] L. M, A. S, H. W, Differential analysis of count data–the DESeq2 package, Genome Biol. 15 (550) (2014) 10–1186.
[22] J.A. Ferreira, S.O. Nyangoma, A multivariate version of the Benjamini–Hochberg method, J. Multivariate Anal. 99 (2008) 2108–2124.
[23] P. Wang, Y. Wang, B. Hang, X. Zou, J.H. Mao, A novel gene expression-based prognostic scoring system to predict survival in gastric cancer, Oncotarget 7 (2016) 55343–55351.
[24] R. Tibshirani, The lasso method for variable selection in the Cox model, Stat. Med. 16 (1997) 385–395.
[25] F.E. Harrell Jr., M.F.E. Harrell Jr., H. D, Package "rms, Vanderbilt University, 2017, p. 229.
[26] P. Geeleher, N. Cox, R.S. Huang, pRRophetic: an R package for prediction of clinical chemotherapeutic response from tumor gene expression levels, PLoS One 9 (2014) e107468.
[27] D. Kazandjian, Multiple myeloma epidemiology and survival: a unique malignancy, Semin. Oncol. 43 (2016) 676–681.
[28] B.Q. Yang, J.M. Chen, Z.Y. Zeng, [Research progress on regulating autophagy in the treatment of multiple myeloma –Review], Zhongguo Shi Yan Xue Ye Xue Za Zhi 28 (2020) 700–703.
[29] Y. Lu, Y. Wang, H. Xu, C. Shi, F. Jin, W. Li, Profilin 1 induces drug resistance through Beclin1 complex-mediated autophagy in multiple myeloma, Cancer Sci. 109 (2018) 2706–2716.
[30] M.E. Murray, C.M. Gavile, J.R. Nair, C. Koorella, L.M. Carlson, D. Buac, A. Utley, M. Chesi, P.L. Bergsagel, L.H. Boise, K.P. Lee, CD28-mediated pro-survival signaling induces chemotherapeutic resistance in multiple myeloma, Blood 123 (2014) 3770–3779.
[31] X.Y. Wen, S. Mandelbaum, Z.H. Li, M. Hitt, F.L. Graham, T.S. Hawley, R.G. Hawley, A.K. Stewart, Tricistronic viral vectors co-expressing interleukin-12 (IL-12) and CD80 (B7-1) for the immunotherapy of cancer: preclinical studies in myeloma, Cancer Gene Ther. 8 (2001) 361–370.
[32] I.R. Ramachandran, T. Condamine, C. Lin, S.E. Herlihy, A. Garfall, D.T. Vogl, D.I. Gabrilovich, Y. Nefedova, Bone marrow PMN-MDSCs and neutrophils are functionally similar in protection of multiple myeloma from chemotherapy, Cancer Lett. 371 (2016) 117–124.
[33] T. Hoshino, M. Okamoto, Y. Sakazaki, S. Kato, H.A. Young, H. Aizawa, Role of proinflammatory cytokines IL-18 and IL-1β in bleomycin-induced lung injury in humans and mice, Am. J. Respir. Cell Mol. Biol. 41 (2009) 661–670.
[34] Y.Q. Sun, Q.F. Li, Q.K. Zhang, X.F. Wei, Y.F. Feng, [Significance of neutrophil/lymphocyte ratio in the prognosis of patients with multiple myeloma], Zhongguo Shi Yan Xue Ye Xue Za Zhi 27 (2019) 489–493.
[35] S. Zhu, Q. Wu, B. Zhang, H. Wei, B. Li, W. Shi, M. Fang, S. Zhu, L. Wang, Y. Lang Zhou, Y. Dong, Autophagy-related gene expression classification defines three molecular subtypes with distinct clinical and microenvironment cell infiltration characteristics in colon cancer, Int Immunopharmacol 87 (2020) 106757.
[36] L. Zhang, J.Y. Qi, P.J. Qi, Y.F. Wang, D.H. Zou, H.J. Yao, G. An, S.H. Yi, Q. Li, L.G. Qiu, Comparison among immunologically different subtypes of 595 untreated multiple myeloma patients in northern China, Clin Lymphoma Myeloma Leuk 10 (2010) 197–204.
[37] R. Zhou, A.S. Yazdi, P. Menu, J. Tschopp, A role for mitochondria in NLRP3 inflammasome activation, Nature 469 (2011) 221–225.
[38] R. Lu, Q. Zhou, L. Ju, L. Chen, F. Wang, J. Shao, Upregulation of TRIP13 promotes the malignant progression of lung cancer via the EMT pathway, Oncol. Rep. 46 (2021).
[39] D. Barakeh, E. Faqeih, S. Anazi, S.A.-D. M, A. Softah, F. Albadr, H. Hassan, A.M. Alazami, F.S. Alkuraya, The many faces of KIF7, Hum Genome Var 2 (2015) 15006.
[40] K.Y. Wong, J. Liu, K.W. Chan, KIF7 attenuates prostate tumor growth through LKB1-mediated AKT inhibition, Oncotarget 8 (2017) 54558–54571.
[41] J.B. Regard, I.T. Sato, S.R. Coughlin, Anatomical profiling of G protein-coupled receptor expression, Cell 135 (2008) 561–571.
[42] X. Huang, Y. Wang, X. Nan, S. He, X. Xu, X. Zhu, J. Tang, X. Yang, L. Yao, X. Wang, C. Cheng, The role of the orphan G protein-coupled receptor 37 (GPR37) in multiple myeloma cells, Leuk. Res. 38 (2014) 225–235.

[43] J. Loc'h, M. Delarue, Terminal deoxynucleotidyltransferase: the story of an untemplated DNA polymerase capable of DNA bridging and templated synthesis across strands, Curr. Opin. Struct. Biol. 53 (2018) 22–31.
[44] R. Cristofani, M. Piccolella, V. Crippa, B. Tedesco, M. Montagnani Marelli, A. Poletti, R.M. Moretti, The Role of HSPB8, a Component of the Chaperone-Assisted Selective Autophagy Machinery, vol. 10, Cancer, 2021. Cells.
[45] M. Piccolella, V. Crippa, R. Cristofani, P. Rusmini, M. Galbiati, M.E. Cicardi, M. Meroni, N. Ferri, F.F. Morelli, S. Carra, E. Messi, A. Poletti, The small heat shock protein B8 (HSPB8) modulates proliferation and migration of breast cancer cells, Oncotarget 8 (2017) 10400–10415.
[46] M.A. Hamouda, N. Belhacene, A. Puissant, P. Colosetti, G. Robert, A. Jacquel, B. Mari, P. Auberger, F. Luciano, The small heat shock protein B8 (HSPB8) confers resistance to bortezomib by promoting autophagic removal of misfolded proteins in multiple myeloma cells, Oncotarget 5 (2014) 6252–6266.
[47] N.F. Pondé, D. Zardavas, M. Piccart, Progress in adjuvant systemic therapy for breast cancer, Nat. Rev. Clin. Oncol. 16 (2019) 27–44.
[48] Brandt, J.P., Gerriets, V., 2022. Bleomycin. In StatPearls. Vol., ed.ˆeds. StatPearls Publishing Copyright © 2022, StatPearls Publishing LLC., Treasure Island (FL).
[49] Z. Wu, Z. Lu, L. Li, M. Ma, F. Long, R. Wu, L. Huang, J. Chou, K. Yang, Y. Zhang, X. Li, G. Hu, Y. Zhang, C. Lin, Identification and validation of ferroptosis-related LncRNA signatures as a novel prognostic model for colon cancer, Front. Immunol. 12 (2021) 783362.
[50] Y. Wang, Q. Shao, S. Luo, R. Fu, Development of a nomograph integrating radiomics and deep features based on MRI to predict the prognosis of high grade Gliomas, Math. Biosci. Eng. 18 (2021) 8084–8095.
[51] W. Zhang, L. Ji, X. Wang, S. Zhu, J. Luo, Y. Zhang, Y. Tong, F. Feng, Y. Kang, Q. Bi, Nomogram predicts risk and prognostic factors for bone metastasis of pancreatic cancer: a population-based analysis, Front. Endocrinol. 12 (2021) 752176.
[52] Z.L. Hou, Y. Kang, G.Z. Yang, Z. Wang, F. Wang, Y.X. Yu, W.M. Chen, H.Z. Shi, Pleural effusion-based nomogram to predict outcomes in unselected patients with multiple myeloma: a large single center experience, Ann. Hematol. 100 (2021) 1789–1801.
[53] Y. Zhang, X.L. Chen, W.M. Chen, H.B. Zhou, Prognostic nomogram for the overall survival of patients with newly diagnosed multiple myeloma, BioMed Res. Int. 2019 (2019) 5652935.
[54] H.L. Chen, C.C. Ma, Y. Chai, P.Y. Zeng, C.Y. Wu, L.L. Yue, T.Y. Han, D.K. Zhang, [A prognostic nomogram based on response to bortezomib and BTK expression for treatment-experienced multiple myeloma patients], Zhongguo Shi Yan Xue Ye Xue Za Zhi 30 (2022) 1139–1143.
[55] W. Wang, S.W. Xu, X.Y. Zhu, Q.Y. Guo, M. Zhu, X.L. Mao, Y.H. Chen, S.W. Li, W.D. Luo, Identification and validation of a novel RNA-binding protein-related gene-based prognostic model for multiple myeloma, Front. Genet. 12 (2021) 665173.